Robust Cell Image Segmentation Methods[1]

E. Bengtsson, C. Wählby, and J. Lindblad

Center for Image Analysis, Uppsala University, Lägerhyddsv. 3, Uppsala, 75235 Sweden
e-mail: ewert@cb.uu.se

Abstract—Biomedical cell image analysis is one of the main application fields of computerized image analysis. This paper outlines the field and the different analysis steps related to it. Relative advantages of different approaches to the crucial step of image segmentation are discussed. Cell image segmentation can be seen as a modeling problem where different approaches are more or less explicitly based on cell models. For example, thresholding methods can be seen as being based on a model stating that cells have an intensity that is different from the surroundings. More robust segmentation can be obtained if a combination of features, such as intensity, edge gradients, and cellular shape, is used. The seeded watershed transform is proposed as the most useful tool for incorporating such features into the cell model. These concepts are illustrated by three real-world problems.

1. INTRODUCTION

1.1. Image Analysis in Cancer Research

One of the first and largest application fields for image analysis is biomedicine in general and, particularly, pathology. The final diagnostic decision for many diseases is based on microscopic examination of cells and tissues. In particular, cancer is always finally diagnosed through the microscope. If cell samples from healthy individuals can be examined, precursors of cancer can be detected even before they develop into the dangerous disease and cured by simple means. The most prominent example is screening for cervical cancer through the so-called pap smear, which has significantly reduced the incidence and mortality of the second most common type of cancer for women in countries with an effective screening program [5]. The visual interpretation is, however, tedious and in many cases error-prone. Therefore, ever since the first appearance of computers, significant development efforts have been aiming at supplementing or replacing human visual inspection with computer analysis [4].

In addition to its diagnosis and screening applications, microscopic examination can help in grading the cancer, i.e., to determine how aggressive it is and how it should be treated. The grading may be based on an assessment of the amount of DNA per cell nucleus, studying the deviation from the normal chromosomal chromatin content. It may also be based on specific staining of some other marker, e.g., associated with cell proliferation. Here, various immunostaining techniques have been developed. Computerized image analysis may be used to automatically measure the staining reaction in a quantitative way. In these applications, the superior capability of the computer to count and measure the number of stained objects and their area is of great value [28].

The grading can also be based on a study of the organization of the tissue, sometimes called cellular sociology. Here, the pathologist is judging the degree to which the cancer has caused the natural order and structure in the tissue to break down. Finding all the cells in a tissue sample and then describing their relative distances, orientations, etc., through graph analysis, the computer can generate a grading that is similar to that of the pathologist but in a more quantitative and, hopefully, more objective and reproducible way [12].

1.2. Cytomics

Even though the cancer-related applications of cell image analysis have been dominating, there are several other important applications within the field. There have been very interesting developments of automated blood cell differential counters with many generations of machines appearing over the years. And similarly, there have been substantial developments in the field of computer-assisted chromosome analysis systems. Today, the rapid development in modern bioscience is opening a whole new application field for tools that have been developed for cancer cell image analysis over the last decades.

The well-known HUGO project led to an almost complete map of the human genome, and significant efforts are currently focused on mapping what proteins the different genes express. In order to completely understand the functioning of the cells and organs of the body, it is also necessary to map when and where the different genes are activated. Cytomics is the science of cell-based analysis that integrates genomics and proteomics with the dynamic function of cells and tissues. Many people regard functional genomics, or cytomics, as the next great challenge for bioscience.

[1] This paper was submitted by the authors in English.

Received December 16, 2003

Pattern Recognition and Image Analysis, Vol. 14, No. 2, 2004, pp. 157–167.

Most of the previous work on mapping genes and protein expressions has been done in bulk, without the possibility of linking the events to specific positions and functions in the cells. In order to move on to deeper understanding of the cell development and behaviors, new microscopy methods will be at the core of developments.

One of the main goals of functional genomics, proteomics, and cytomics is to understand how the cells develop and differentiate from stem cells into highly specialized organ cells, to understand how and when the genes are expressed in the cell, and how the signaling inside and between cells works. Similarly to the case of cancer research, we thus need to study the cells on several levels of resolution, ranging from the intracellular molecular and signaling levels to the population behavior levels. Let us outline a few current examples.

1.3. Time-Lapse Microscopy and Cell Migration Modeling

In order to study and control stem cell multipotency and self-renewal, the cell migration and cell division have to be modeled. This is done by tracking individual cells over time. Image sequences are acquired using time-lapse microscopy supplemented by an incubator system to keep the cells alive and a motorized stage to make it possible to investigate and compare multiple cell cultures, e.g., manipulated cells and controls. Tracking the cells in these sequences presents a number of image analysis challenges. Cells may touch, overlap, or enter or leave the microscopic field of view, as well as divide or die during the time-lapse experiment. The robustness and accuracy of automated tracking methods can be improved if statistical *a priori* information on typical cell movement patterns can be incorporated into the tracking algorithm [11].

1.4. Analysis of Subcellular Compartments and Transportation

Cells are elaborately subdivided into functionally distinct, membrane-bounded compartments. Each compartment contains its own characteristic set of specialized molecules, and complex distribution systems transport specific products from one compartment to another or from one compartment and out of the cell. Proteins catalyze reactions within compartments and selectively transport molecules between compartments. Signals from outside the cell can also trigger specific transport within, as well as into and out of, the cell, e.g., resulting in the secretion of insulin from cells of the pancreas.

By tracking the protein traffic from one compartment to another, a better understanding of the maze of intracellular membranes and signals can be achieved. Specific proteins within living cells can be tagged with green fluorescent protein (GFP), and similar tags, by genetic engineering. The localization and movement of the tagged protein can thereafter be imaged using fluorescence microscopy. Corresponding studies on other types of tagged biomolecules, such as metabolites, can also be performed. Specific intracellular compartments and structures can also be visualized by immunofluorescence staining. The analysis of these signals can often be described as the analysis of fluorescent "blobs." Methods for the detection, characterization, quantification, and positioning of blobs are required. Specialized segmentation methods, as well as methods for the tracking and extraction of features describing morphology, are needed. In addition to their use in basic bioscience research, these kinds of methods are also of great interest to the pharmaceutical industry in the development of new drugs [19].

1.5. Image Analysis Steps

In the development of computerized cell image analysis, there are several important steps that need to be implemented, such as preparing suitable specimens, loading, positioning, and focusing the specimens in the microscope, digitizing an image with suitable resolution and spectral properties, finding areas of interest for the analysis, segmenting the images, extracting useful features, and finally recognizing the diagnostic or other information of interest through classification or pattern recognition techniques on the cellular or specimen level. Each of these steps gives rise to a number of challenging research questions that have been studied in great detail over the half century that has passed since the first achievements in the field took place. If the goal is to create an interactive system, some of the difficulties can be left to the human operator to solve, but when the goal is a fully automated analysis system, all the steps need to be addressed. In a couple of recent papers, we outlined the development of the field over the years [4, 5] and discussed the feature extraction aspects in detail [29]. In this paper, we concentrate on the crucial image-segmentation step.

2. IMAGE-SEGMENTATION MODELS

Segmentation is the process of dividing an image into its constituent objects, or parts, and a background. It is often one of the most important and most difficult steps in an image analysis task. The result of segmentation usually determines eventual success of the final analysis. For this reason, many segmentation techniques have been developed by researchers worldwide and there exist almost as many segmentation methods as there are segmentation problems. The difficulty of the segmentation problem highly depends on the type of specimen to be analyzed. If we are dealing with cytological specimens where the cells are singly lying on a clean background with well-stained nuclei, and if the analysis task is limited to nuclear properties, then a simple automatic thresholding method may be sufficient. If, on the other hand, the cells are presented in

intact tissue, such as histopathological tissue sections, and the nuclei as well as the cytoplasms are stained, then the segmentation task may be difficult indeed. Sometimes, it is necessary to use interactive techniques in order to obtain sufficient data quality. But even in these cases, it is useful to push the automated segmentation as far as possible. Compared to manual methods based on drawing the outlines of the nuclei, computer-aided methods need far less interaction and the result is more objective and easily reproduced. Automation also increases the amount of data that can be processed.

The robustness and power of a segmentation technique is related to the quality of its model of the image that is to be analyzed. If we simply use the fact that the objects are darker than the background, a simple thresholding may work, but the method will be unable to resolve cluttered images with many different types of objects with different densities. If, on the other hand, we have a model that knows the typical density range, edge contrast properties, and the shape of the objects of interest, we can use much more sophisticated methods, e.g., active shape models [13]. But there is a price to pay. The segmentation will fail if the objects in the image do not match the assumed model sufficiently well, or the method may find objects even where there are none. Also, developing very specific models is tedious. So, there is a trade-off: the ideal solution should model as much of the information known about the objects as possible in sufficiently general terms to make it easy to train for a new class of images, but still with sufficient specificity to really find objects of interest and discriminate against unwanted objects and artifacts.

2.1. Different Types of Microscopy

There are several microscopy techniques that are used in cell image analysis. If the cells are to be studied while they are alive, it is better to avoid staining altogether. Interference contrast microscopy can then be used to obtain images of the cells. The process generates images that have similarities with gradient images of stained cells; i.e., they show most contrast where there are spatial changes in the amount of cellular material.

The most widely used technique is transmission, absorption microscopy, where the stains absorb light passing through the specimen. Examples are the Feulgen stain, which stoichiometrically stains DNA, and the stain cocktail developed by Papanicolau and used for staining the hundreds of millions of pap smears analyzed every year. Absorption microscopy images show dark objects against a clear background.

A third imaging method that has become increasingly popular is fluorescence microscopy, where the stains are excited by a shorter wavelength and then emit light at another, longer wavelength. Thus, they have inverted contrast; i.e., the cells are bright against a dark background. One reason for the increased popularity of fluorescent staining techniques is the development of laser scanning microscopes where, through confocal optics or multiphoton excitation, 3D images of tissue sections can be obtained. Fluorescent stains that can be used on living cells without killing the cells have also been developed.

Each type of microscopy poses its own segmentation problems. So far, no general standard solution to the segmentation problem has been found. A new tailored solution is typically developed for each application problem. Still, these solutions can be discussed in terms of image and object models, i.e., what kind of information in the images they are based on and whether it is mainly intensity, edges, connectivity, or shape. Through such a discussion, some general properties can be seen and, hopefully, some useful steps towards more generally useful segmentation approaches can be taken. In this paper, we present such a discussion. As illustrations, we use experiments carried out in our laboratory over past years.

2.2. Thresholding

A simple and often used method for image segmentation is thresholding based on histogram characteristics of the pixel intensities of the image. Here, it is implied that objects of interest are brighter or darker than other parts of the image. For an overview of thresholding techniques, see [32]. In order to get a satisfactory segmentation by thresholding, a sufficiently uniform background is required. Many background correction techniques exist (see, e.g., [14, 18]), but they may not always result in an image suitable for further analysis by thresholding. The transition between object and background may be diffuse, making an optimal threshold level difficult to find. At the same time, a small change in the threshold level may have a great impact on further analysis. Feature measures, such as area, volume, mean pixel intensity, etc., directly depend on the threshold. These effects can be reduced through the use of fuzzy techniques, e.g., fuzzy feature measures [34]. Adaptive thresholding, i.e., local automatic thresholding, can be used to circumvent the problem of varying background or to refine a coarse global threshold [24]. The problems of segmenting clustered objects and choosing a suitable threshold level for objects with unsharp edges will, however, remain. Thresholding does not have to be the final step in the segmentation procedure. An intensity threshold can be used as a start for further processing, e.g., by the morphological operations presented below and/or visual inspection.

2.3. Region Growing

If we model the objects as consisting of connected regions of similar pixels, we obtain region growing methods. The name comes from the fact that starting

regions grow by connecting neighboring pixels/voxels of similar gray level.

Many region-growing algorithms result in oversegmented images; i.e., too many object regions are formed. In [26], region growing is combined with region merging based on edge information, and in [17], the images are preprocessed with an adaptive anisotropic filter to reduce oversegmentation. The adaptive anisotropic filter reduces noise in homogeneous regions while sharpening discontinuities. Using these methods, one is still left to face the prominent clustering problem, i.e., finding separation lines when no intensity variation is present. Another approach, described in [1], is to let the regions grow from predefined small regions, known as seeds. Each region in the resulting segmented image will contain exactly one of the starting seeds. Both manually marked seeds and an automatic seeding method are described. The problem with this approach to cell nuclei segmentation is that it is very difficult to construct a seeding method that puts exactly one seed in each nucleus, even when the nuclei are clustered and/or have internal intensity variations.

2.4. Seeded Watershed Segmentation

A popular region-growing method, which has proved very useful in many areas of image segmentation and analysis, is the so-called watershed algorithm. The method was originally suggested by Digabel and Lantuéjoul and extended to a more general framework by Lantuéjoul and Beucher [7]. Watershed segmentation has then been refined and used in very many situations (for an overview, see [22, 38]). The main difference between the watershed algorithm and ordinary region growing is that the watershed algorithm works per intensity layer instead of per neighbor layer. If the intensity of the image is interpreted as elevation in a landscape, the watershed algorithm will split the image into regions similar to the drainage regions of this landscape. The watershed borders will be built at the crests in the image. In a gradient magnitude image, water will start to rise from minima representing areas of low gradient, i.e., the interior of the objects and the interior of the background, and the watershed borders will be built at the maxima of the gradient magnitude. However, if watershed segmentation is applied directly to the gradient magnitude image, it will almost always result in oversegmentation, due to the intensity variations within both the objects and background.

Instead of letting water rise from every minimum in the image, water can be allowed to rise only from places marked as seeds. Seeded watersheds have previously been described, for example, in [6, 15, 20, 22, 38]. Fully automatic foreground seeding is tricky, and when using morphological filtering, one often ends up with more than one seed per object or objects containing no seed at all. More than one seed per foreground object in many methods, e.g., in [22], results in background seeds passing through foreground components, which leads to incorrect segmentation results. Many seeded watershed segmentation methods are, therefore, based on manual seeding (see, e.g., [20]), requiring extensive user interaction. In [37], a way of using a seeded watershed for extracting a single, manually seeded, region of interest is presented. It uses four merging criteria to overcome the oversegmentation problem. The threshold values needed for the merging step are all calculated from the marked seed in the region of interest. The use of merging to reduce oversegmentation is also described in [16, 23].

2.5. Edge-Based Segmentation

Another observation used as a basis for segmentation is that cells are surrounded by edges where the intensity changes rapidly. Edges are usually initially extracted as a gradient image in which the local maxima are connected. A drawback of this method is that one often runs into problems when trying to produce closed curves. A powerful solution to this problem is offered by the so-called snakes or active shape models [13]. From a rough marking of the border or a seed inside the object of interest, a curve expands until it finds a strong edge. The function describing the expansion consists of different energy terms attracting the curve to edges [25]. Problems with this model consist in defining suitable energy terms and, again, constructing automatic seeding methods that are restricted to one unique seed per nucleus.

Cell nuclei are usually convex and fairly round or elliptic. The shape of the cell nuclei itself can, therefore, be used as part of the object model. In [42], a 3D blob segmentation method based on elliptic feature calculation, convex hull computations, and size discrimination is described. Careful choice of a scale parameter is needed, and the edges of the resulting objects will not necessarily be aligned with the edges of the nuclei. A restricted convex hull is computed for slicewise 3D segmentation in [3]. Distance information in the restricted convex deficiency defines the location of separating lines between clustered objects. The information obtained per slice is later joined to construct 3D objects. Watershed segmentation applied to distance transformed binary images (usually binarized through thresholding) is useful for separating touching objects that are convex (see [21, 24, 41]). In [14], similar separating lines between touching objects are found in a slightly different way. The distance image is thresholded, creating a new binary image consisting of shrunk versions of all the objects. Dividing lines are thereafter defined as the skeleton of the background of this binary image.

2.6. Combined Seeded Watershed Models

None of the above-described methods will alone produce a satisfactory result on the more difficult types

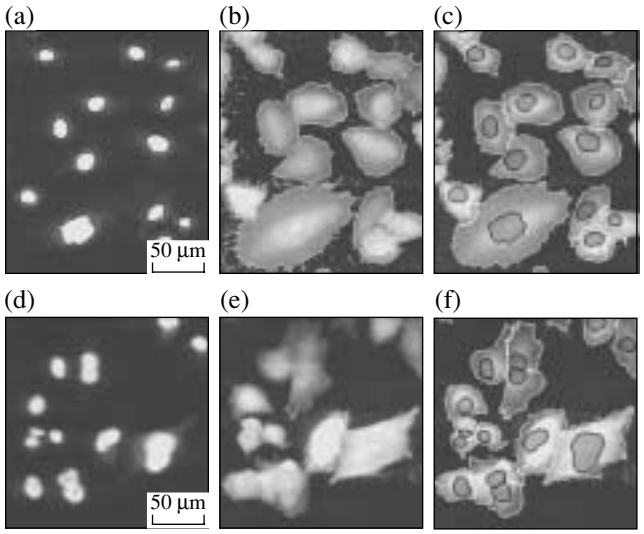

Fig. 1. Segmentation results: (a) segmentation of the nuclei is seen as black borders outlining the nuclei; (b) thresholding of the cytoplasm image (white borders) does not separate the individual cells; (c) if the nuclei (darker regions with black borders) are used as seeds for watershed segmentation of the cells, all cells are separated (white borders); (d–f) a difficult region: (d) clustered nuclei and (e) overlapping cytoplasms; (f) the resulting segmentation is shown.

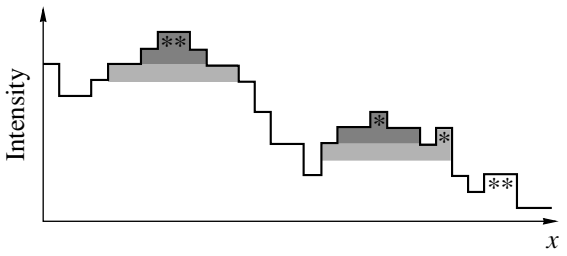

Fig. 2. *h*-Maxima in 1D. The local maxima in the 1D image, or intensity profile, are marked by stars and represent the result of *h*-maxima transformation using $h = 1$. If $h = 2$ or $h = 3$, the result will be the dark or light gray regions, respectively. A low *h* will result in many small regions, while a larger *h* will result in fewer but larger regions.

of cell and tissue images. We may, for instance, have problems if (i) the cells are clustered, (ii) the image background varies, and (iii) there are intensity variations within the cells. By combining the methods, more powerful models of the situation can be created which can solve many segmentation problems. Our experience has shown that the seeded watershed approach is a useful core component in such more complex segmentation models. In the next section, we will briefly outline a few illustrative examples.

3. EXPERIMENTS AND RESULTS

To illustrate the concepts discussed so far in this paper, we briefly describe three projects where we successfully applied combined seeded watershed models for cell image segmentation.

3.1. Living Cells in Culture

Drugs are often synthetic molecules that affect the dynamic events in individual cells. By studying cells over time and exposing them to drugs, important information about the applied drugs can be retrieved. Analysis of single cells can thus be used as a screening step in the search for new drugs. High-throughput screening requires fast and fully automatic methods for single cell analysis.

The basis for all automated image cytometry is cell segmentation. Before any cell-specific spatial, spectral, and temporal features can be extracted, the individual cells have to be segmented from the image background and from each other. While the nuclei of the cells are often quite distinct and easy to detect, e.g., based on their regular shape [21, 28], the cells are a lot more challenging. If we need to segment both whole cells and nuclei, we can model a cell as containing a nucleus surrounded by a cytoplasm. We have recently developed a fully automatic image analysis method for quantifying ruffle formation, i.e., formations associated with GFP-Rac1 translocation in individual cells.

Evaluation of ruffling in individual cells requires outlining cytoplasm of each cell, i.e., cytoplasm segmentation. Apart from expressing the GFP-Rac1, which shows a green fluorescence, the cells were also stained with Hoechst™ 33258, a blue nuclear marker. This image of the cell nuclei was first segmented, and the result was used as seeds to simplify the segmentation of the cytoplasms [19]. See illustration in Fig. 1.

3.1.1. Seeding by segmentation of nuclei. Each cell contains one nucleus, and by firstly segmenting the nuclei and using them as seeds in watershed segmentation of the cells, cytoplasm segmentation is simplified. This approach certainly requires a dual staining technique where the nuclei can be detected and segmented first. This is, however, the case in many applications. The nuclei were separated from the background by an image-specific intensity threshold. The threshold was automatically set, so that the contrast between border pixels belonging to object and background was maximized. After thresholding, clustered nuclei had to be separated. A distance image was created by applying the Euclidean distance transform to the binary objects [9]. Touching circular nuclei were thereafter separated by applying watershed segmentation to the distance image [27, 39]. The result of the nuclear segmentation can be seen in Figs. 1a, 1c, and 1f.

3.1.2. Segmentation of cells. The whole cytoplasm of each cell has to be delineated to know what pixels (ruffles, intensities, etc.) are associated with each cell. The cells were separated from the image background using the foreground–background intensity threshold found by a spline-based preprocessing step [10, 18].

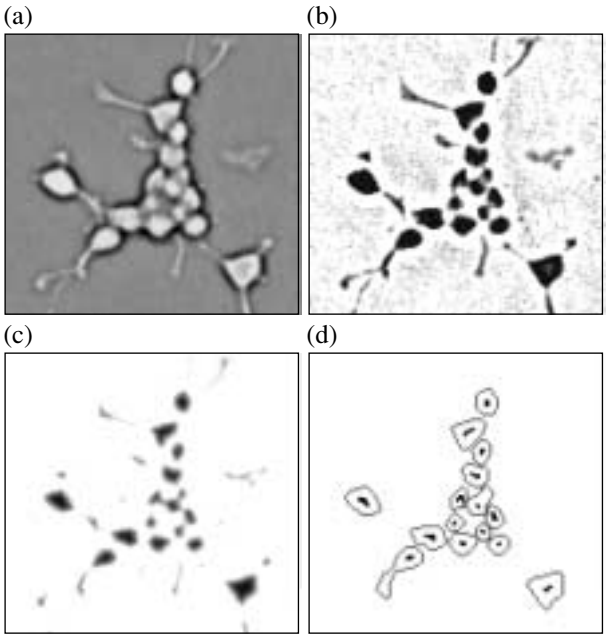

Fig. 3. Segmentation of cells. Shown is a small part of one image in a time sequence. (a) Original image; (b) fuzzy thresholded image; (c) result after applying the fuzzy distance transform; (d) seeds (black) and region borders (gray) of the resulting watershed segmentation.

Touching cells are, however, not separated by simple thresholding (see Fig. 3b). Instead, the cells can be separated using watershed segmentation [6, 39]. Each seed, i.e., nucleus, will give rise to a catchment basin, and when the water rising from two different seeds meet, a watershed, or border, is built in the image landscape. All pixels associated with the same seed belong to the same cytoplasm, which corresponds to a model where each cell should contain one nucleus.

Watershed segmentation separates touching cells where the border between them is the darkest (i.e., brightest in the negative image). This is a reasonable assumption at time 0, when the GFP-Rac1 is evenly spread in the cytoplasm. After addition of agonist, the signal is less smooth and the borders between the cytoplasms tend to be brighter due to the GFP-Rac1 translocation. Applying watershed segmentation to these images may, therefore, position the cell borders incorrectly. Robust analysis of GFP-Rac1 translocation requires well-defined cell borders also after adding agonist. One approach is to use the segmentation result from time 0 as a mask, but cell motion and shape changes result in an unreliable segmentation. The changes in shape and position are compensated for by first thresholding the images in the same manner as for time 0. The segmentation result from time 0 is thereafter allowed to grow within the Voronoi region [2] associated with each cell, i.e., the region that is not closer to any other cell.

3.1.3. Feature extraction. Once each cell has been outlined, a number of features have to be defined and extracted from the image data. The combination of the extracted feature values for a cell is the basis for classifying this cell as showing no, moderate, or high activation, and should describe the accumulation of GFP-Rac1 at the cytoplasmic membrane. There exist thousands of different features in the literature, and the choice of features to include in the classification process is not trivial. More features are not always better [33]. We, therefore, restricted the search for good features to those that are intuitively felt to be related to the biological process we wanted to describe. We also created a number of problem-specific features specially designed to capture the ruffling formation.

3.1.4. Results. Segmentation of cytoplasms by using a parallel image showing the cell nuclei as seeds proved to be very successful and not a limiting factor in the classification of cells according to their activation. The limiting factor was instead the feature extraction and the training of the classifier. Final classification results were similar to those obtained by visual classification, and the variability between a visual classification and the fully automated computer-based classification was about the same as the variability between visual classifications performed by two different persons.

3.2. Cell Nuclei in Tissue

A difficult case, where no separately defined seeds are available, is fluorescent images of cell nuclei in tissue. Images of cell nuclei in tissue produced by fluorescence microscopy often show an uneven background intensity due to autofluorescence from the tissue and fluorescence from objects that are out of focus. This unevenness makes the separation of foreground and background nontrivial. Intensity variations within the nuclei, as well as clustered nuclei, further complicate the segmentation. We propose a region-based method where seeds representing object- and background-pixels are created by combining morphological filtering of both the original image and the gradient magnitude of the image. The seeds are then used as starting points for watershed segmentation of the gradient magnitude image.

3.2.1. Seeding. Seeds marking probable foreground and background regions are planted in the image. These seeds serve as starting points in the watershed algorithm applied to the gradient magnitude image. In the case of fluorescence stained cell nuclei, the images contain bright objects against a darker background. Hence, each object of interest contains at least one local intensity maximum. We define foreground seeds in the original image using the extended h-maxima transform [35]. The extended h-maxima transform filters out the relevant maxima using a contrast criterion. All maxima whose heights are smaller than a given threshold level h are suppressed (see Fig. 2). A high h will result in

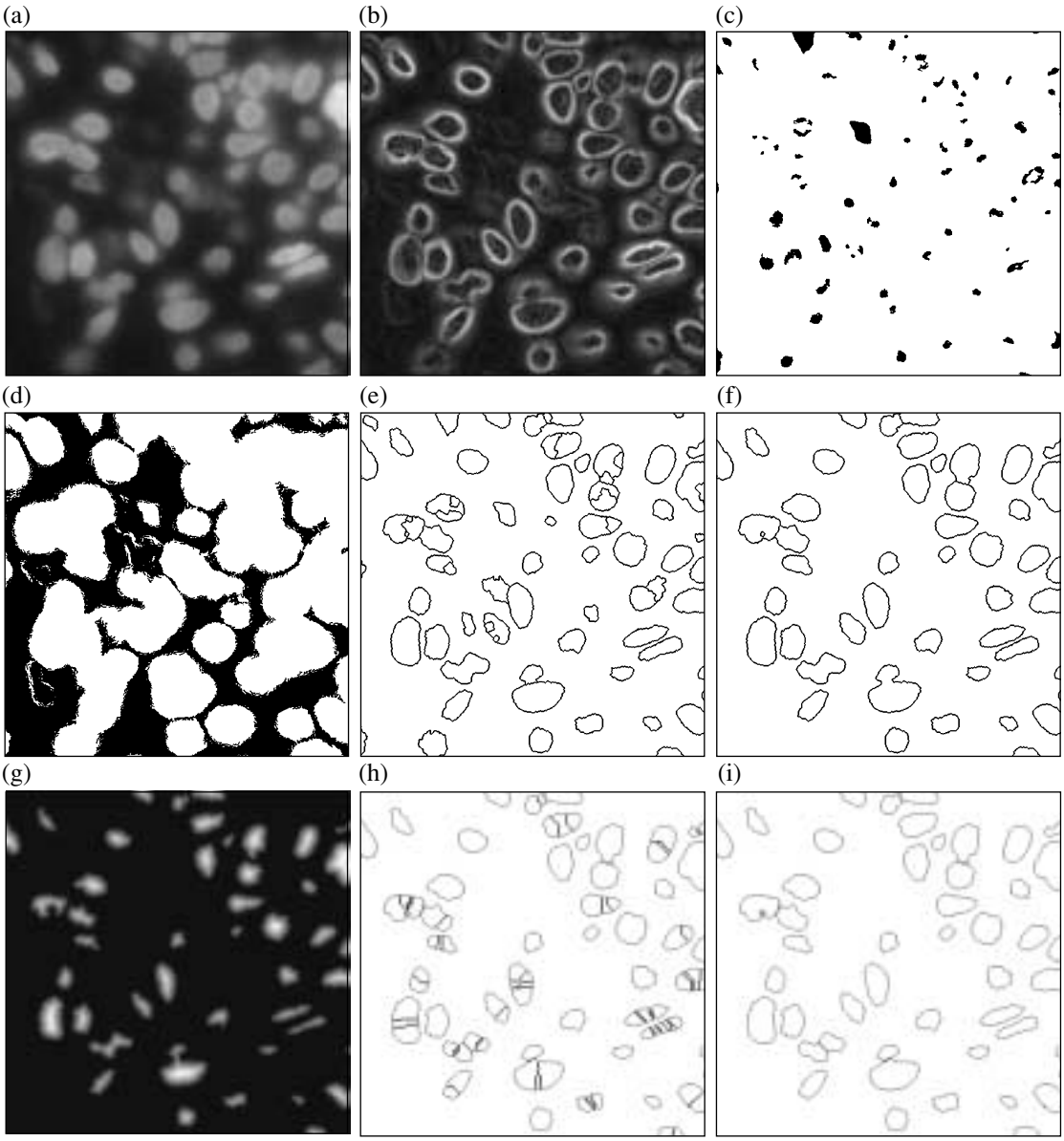

Fig. 4. (a) Part of an original fluorescence microscopy image of a slice of a tumor; (b) the gradient magnitude of (a); (c) the foreground seeds found by extended *h*-maxima transformation; (d) the background seeds found by extended *h*-maxima transformation of the gradient magnitude image followed by removal of small components; (e) result of seeded watershed segmentation; (f) the result after merging seeded objects based on edge strength (poorly focused objects are also removed in this step); (g) the distance transform of the objects in the segmented image (the brighter the intensity, the further the pixel from the background or a neighboring object); (h) watershed segmentation of the distance transform before merging; (i) final segmentation result based on intensity, edge, and shape information.

fewer seeds, and some objects may not get a seed at all. Due to a subsequent merging step based on gradient magnitude (described below), we use a rather low *h* value to make sure that each object gets at least one seed. The result is shown in Fig. 4c.

The background can be seeded by extended *h*-minima in the original image, i.e., local minima deeper than a certain depth *h*. As the background intensity is generally higher close to fluorescent objects, this way of seeding generates very few background seeds close to the objects. We choose to define the background seeds in the gradient magnitude image instead. We calculate the gradient magnitude image, as described below, and define our background seeds as the extended *h*-minima in the gradient magnitude image. Since the interiors of cell nuclei also will be local minima in the gradient magnitude (see Fig. 4b), we have to discard all connected extended *h*-minima components smaller than a certain size *s* to make sure that no object pixels are set as background seeds. This way of using the gradient

magnitude image to seed the background generates background seeds evenly distributed in the image, even if an image has a nonuniform background. The final background seeds can be seen in Fig. 4d.

3.2.2. Gradient-based watershed segmentation. The seeds of the objects and the seeds of the background should grow and meet where the gradient magnitude image has a local maximum. The magnitude of the gradient expresses the variation of local contrast in the image; i.e., sharp edges have a high gradient magnitude, while more uniform areas in the image have a gradient magnitude close to zero. The local maximum of the gradient amplitude marks the position of the strongest edge between object and background. There exist many different approximations of the gradient magnitude of an image. The most popular is the Sobel operator, and since it works well in this application we use it [36]. The resulting gradient magnitude can be seen in Fig. 4b. In our seeded version of the watershed segmentation, water will rise from pixels marked as seeds, as well as from nonseeded regional minima found in the image. Separating dams, or watersheds, are built only between catchment basins associated with different seeds. As soon as the water level of a seeded catchment basin reaches the weakest point of the border towards a nonseeded regional minimum, it will be flooded. The water will continue to rise until each seeded catchment basin in the gradient magnitude image meets another seeded catchment basin.

3.2.3. Merging regions with weak borders. If too many seeds are created in the seeding step, some objects will have more than one seed. These objects will be oversegmented after the watershed algorithm, since each seed results in one region. However, if two seeds are in the same object, the magnitude of the gradient at the region boundaries will usually be small. The strength of a border separating two regions is calculated as the mean intensity along the border. The mean value of the border of each merged object must be updated after merging, and the merging is continued until all remaining object borders are stronger than a threshold t_e.

A strong border means that the object is well focused. When merging is based on a border strength, not only oversegmented objects are merged, but also poorly focused objects are merged into the background and disappear. This may be useful if well-focused objects are important in further analysis of the fluorescent signals (see, e.g., [40]). In this case, a rather high threshold t_e is suitable.

3.2.4. Separating clusters using shape. Tightly clustered nuclei most likely do not show a strong border where they touch and thus are not properly separated by watershed segmentation. However, as a result of the previous steps, we get a correct segmentation of the clusters from the background. Cell nuclei are usually convex and can be separated from each other based on shape, as previously described in, e.g., [30, 38]. We use the seeded and edge-merged watershed result as a binary input to a distance transformation and, thereafter, apply watershed segmentation to the distance image. The distance transform of a binary image assigns to each object pixel the distance to the closest background pixel. We have used the 3- to 4-distance transform [8] (see Fig. 4g). Taking the inverse of the distance image, the distance maxima serve as regional minima for watershed segmentation. Catchment basins are built around every distance maxima, as shown in Fig. 4h. As the nuclei are fairly round, the most prominent distance maxima coincide with the centers of nuclei and catchment basin borders coincide with the more narrow waists of clusters. The discrete distance image may, however, contain too many local maxima, resulting in oversegmentation. Merging based on the weakest border pixel is applied to reduce this oversegmentation. Only the borders whose minimum strength is greater than t_s are kept, corresponding to a maximal allowed shape variation of the object. The result can be seen in Fig. 4i.

3.2.5. Results. The segmentation method was tested on 2D and 3D images of tissue sections from samples of routinely fixed and paraffin-embedded carcinoma of the prostate as described in [41]. Each image contained 87–133 cells, with 689 cells in total. Once the five input parameters h_{fg}, h_{bg}, s, t_e, and t_s were set for the whole experiment, based on a single training image, the experiments needed no human interaction. The segmentation result achieved by the described method was compared to manual counts from the same image fields. The average agreement was 91%. The small variation in the result shows that the method is robust.

3.3. Bright-Field Images of Stem Cells

Combining shape and intensity with the use of morphological filtering for seed finding proves to be a good solution also when segmenting bright-field microscopy images of cells. In order to track cultured neuronal precursor cells as they differentiate to neurons and glial cells (Fig. 3a), we need a fast and robust segmentation algorithm.

There is a distinction between fluorescence microscopy images and bright-field images. Fluorescent cells emit light, while, in the case of the bright-field microscope, light is absorbed and diffracted by the cells. Due to the presence of a visible background, processing of bright-field images is more complex than that of fluorescent images. However, there are more similarities than differences and problems and solutions here resemble those of the fluorescence studies.

3.4. Image Acquisition

The imaging system used was a Leica™ DM IRB bright-field microscope (20× lens), a Prior™ stage and Solent Scientific™ incubator technology. Cells were cultured in enclosed Falcon™ cell culturing plates with

a carbon dioxide enriched gas supply and a heated environment of 37°C. Since the experiment was run over several days and the illumination conditions did not stay quite stable over that period of time, automatic exposure tuning was required. This was done by computing and evaluating an image histogram for each image.

A focus is a complicated part of imaging. The reason for this is that the size (thickness) of the cell is significant in comparison with the depth of focus. This means that the cell plate cannot be treated as a two-dimensional object. For a specific depth of focus, a specific part of the cell is sharp. To acquire an image of optimal focal properties, we take a stack of images of different focal planes and select the plane where the best contrast is achieved.

3.4.1. Preprocessing. The images acquired suffered from slight variations in intensity over the field of view. Careful calibration of the microscope setup reduced this to a minimum, but additional data-driven processing improved the situation further. We tested three shading-correction methods. The B-spline shading correction method based on the iterative kernel density estimate described in [18] gave good results. Homomorphic filtering with a large average filter gave worse results due to the influence of larger bright clusters of cells. Homomorphic filtering with a large median filter (45×45) gave satisfactory shading correction. We decided to use the median filter approach, since it is significantly simpler than the method presented in [18]. A 3×3 Gaussian smoothing was also performed to reduce noise in images.

The acquired images also had a variation in intensity over time. We therefore normalized the intensity level of the images. Normalizing the intensity over the entire image, i.e., subtracting the mean and dividing by the standard deviation of the pixel intensities, gave fair results. This method is, however, sensitive to the number of cells in the image. Better results were achieved by making a rough foreground/background segmentation and then normalizing only on the base of the background intensities. The initial foreground/background segmentation was done by thresholding the original image at one standard deviation above the mean intensity of the whole image, thus removing the cells. A second better estimate of the overall image intensity is then made from what is below this threshold. The stability of this normalization, of course, requires that the background noise level stays fairly constant over the time of the experiment, which was the case here.

3.4.2. Fuzzy thresholding and seeding. To segment the preprocessed images into individual cells, we perform a fuzzy thresholding, where the intensity range is rescaled to the range [0, 1] (Fig. 3b). The value 0 is set to all pixels with intensity below the lower threshold t_l, and 1 is set to all pixels above the higher threshold t_h. Between t_l and t_h, image intensities are linearly rescaled. t_l is set just above the background level, at $\mu + 0.3\sigma$ of the background (an approximate background is achieved by using the shading correction algorithm). t_h is set at a level of $\mu + 4\sigma$ of the background. This level is high enough to guarantee that pixels brighter than that are really well inside the cells. Due to the use of a fuzzy approach, the method becomes less sensitive to the exact values of these threshold levels than if a standard crisp thresholding had been used.

On the fuzzy thresholded image, we apply a fuzzy/gray weighted distance transform [31] to incorporate both the shape (roundness) and the intensity of the cells (Fig. 3c). This gives us a good landscape to segment by using the watershed algorithm [39]. We again use the extended *h*-maxima transform [35] to find suitable seed points for the watershed algorithm in the fuzzy distance image (Fig. 3d). For an h maximum to be used as a seed for the watershed algorithm, we require its intensity to be above a threshold t_{DT} in the fuzzy distance transformed image. This last threshold enables us to conveniently remove small and faint objects from the image. The watershed segmentation is allowed to grow up to the lower threshold t_l.

3.4.3. Results. The segmentation results for the described method are not absolutely perfect on the rather difficult images that we have been working with: there is some over- and undersegmentation. Since we have a time sequences of images, additional information from the previous and the following image can help us to decide if a cell, e.g., should be split into two. Since the main task of this project is to perform tracking of cells, features are extracted from the segmented cells and this information is then used in a Multiple Hypothesis Tracking scheme employing dynamic programming in order to assign the individual cells of one time frame image to the correct path in the spatiotemporal domain. This work is still under way, but the preliminary results show great promise.

4. DISCUSSION AND CONCLUSIONS

We have discussed the important general problem of cell segmentation, which is a crucial step in most cell image analysis applications. In order to obtain a successful segmentation method, it is important to use as much *a priori* information as possible about the appearance of the objects that are to be segmented, without resorting to models that are too complex or too difficult to train or apply. We propose that models which combine intensity, gradient, connectivity, and shape information using watershed transforms are very useful for creating robust cell image segmentation methods. This approach has solved several difficult real-world segmentation problems, and we believe it will be useful also for many other problems. In our work, so far, we have defined the few necessary input parameters based on a typical training image for each problem. It should be possible to develop ways of doing this fully automatically, since the results are not overly sensitive to the exact values of the parameters.

REFERENCES

1. R. Adams and L. Bischof, "Seeded Region Growing," IEEE Trans. Pattern Anal. Machine Intell. **16** (6), 641–647 (1994).
2. C. Arcelli and G. Sanniti di Baja, "Computing Voronoi Diagrams in Digital Pictures," Pattern Recognit. Lett. **4**, 383–389 (1986).
3. J. A. M. Beliën, H. A. H. M. van Ginkel, P. Tekola, *et al.*, "Confocal DNA Cytometry: A Contour-Based Segmentation Algorithm for Automated Three-Dimensional Image Segmentation," Cytometry **49**, 12–21 (2002).
4. E. Bengtsson, "Fifty Years of Attempts to Automate Screening for Cervical Cancer," Med. Imaging Technol. **17**, 203–210 (1999).
5. E. Bengtsson, "Computerized Cell Image Analysis: Past, Present, and Future," in *Proc. of the 13th Scandinavian Conf. on Image Analysis (SCIA), Lecture Notes in Computer Science, Gothenburg, Sweden, 2003*, Ed. by J. Bigun and T. Gustavsson (Springer, 2003), Vol. 2749, pp. 395–407.
6. S. Beucher, "The Watershed Transformation Applied to Image Segmentation," Scanning Microscopy **6**, 299–314 (1992).
7. S. Beucher and C. Lantuéjoul, "Use of Watersheds in Contour Detection," in *Int. Workshop on Image Processing: Real-time and Motion Detection/Estimation, Rennes, France, September 1979.*
8. G. Borgefors, "Distance Transformations in Digital Images," Comput. Vision Graph. Image Processing, **34**, 344–371 (1986).
9. H. Breu, J. Gil, D. Kirkpatrick, and M. Werman, "Linear Time Euclidean Distance Transform Algorithms," IEEE Trans. Pattern Anal. Machine Intell. **17** (5), 529–533 (1995).
10. S. Gilles, M. Brady, J. Declerck, *et al.*, "Bias Field Correction of Breast MR Images," in *Proc. of the 4th Int. Conf. on Visualization in Biomed. Comput. (VBC), Hamburg, Germany, 1996* (Springer, 1996), p. 153–158.
11. T. Gustavsson, K. Althoff, J. Degerman, *et al.*, "Time-Lapse Microscopy and Image Processing for Stem Cell Research—Modeling Cell Migration," in *Proc. of SPIE, San Diego, USA, 2003*, Vol. X.
12. T. Jarkraans, J. Vasko, E. Bengtsson, *et al.*, Grading of Transitional Cell Bladder Carcinoma by Image Analysis of Histological, Anal. Cell. Pathol. **8**, 135–158 (1995).
13. M. Kass, A. Witkin, and D. Terzopoulos, "Snakes: Active Contour Models," Int. J. Comput. Vision **1**, 321–331 (1988).
14. A. Krtolica, C. Ortiz de Solorzano, S. Lockett, and J. Campisi, "Quantification of Epithelial Cells in Coculture with Fibroblasts by Fluorescence Image Analysis," Cytometry **49**, 73–82 (2002).
15. G. Landini and I. E. Othman, "Estimation of Tissue Layer Level by Sequential Morphological Reconstruction," J. Microscopy **209** (2), 118–125 (2003).
16. C. Lemaréchal and R. Fjortoft, "Comments on 'Geodesic Saliency of Watershed Contours and Hierarchical Segmentation'," IEEE Trans. Pattern Anal. Machine Intell. **20** (7), 762–763 (1998).
17. Z. Lin, J. Jin, and H. Talbot, "Unseeded Region Growing for 3D Image Segmentation," in *Visualization 2000, Pan-Sydney Workshop on Visual Information Processing, 2000*, pp. 31–37.
18. J. Lindblad and E. Bengtsson, "A Comparison of Methods for Estimation of Intensity Nonuniformities in 2D and 3D Microscope Images of Fluorescence Stained Cells," in *Proc. of the 12th Scandinavian Conf. on Image Analysis (SCIA), Bergen, Norway, 2001*, Ed. by I. Austvoll (NOBIM), pp. 264–271.
19. J. Lindblad, C. Wählby, E. Bengtsson, and A. Zaltsman, "Image Analysis for Automatic Segmentation of Cytoplasms and Classification of Rac1 Activation," submitted to Cytometry (September 2003).
20. S. J. Lockett, D. Sudar, C. T. Thompson, *et al.*, "Efficient, Interactive, and Three-Dimensional Segmentation of Cell Nuclei in Thick Tissue Sections," Cytometry **31**, 275–286 (1998).
21. N. Malpica, C. Ortiz de Solorzano, J. J. Vaquero, *et al.*, "Applying Watershed Algorithms to the Segmentation of Clustered Nuclei," Cytometry **28** (4), 289–297 (1997).
22. F. Meyer and S. Beucher, "Morphological Segmentation," J. Visual Commun. Image Representation **1** (1), 21–46 (1990).
23. L. Najman and M. Schmitt, "Geodesic Saliency of Watershed Contours and Hierarchical Segmentation," IEEE Trans. Pattern Anal. Machine Intell. **18** (12), 1163–1173 (1996).
24. C. Ortiz de Solorzano, E. Garcia Rodriguez, A. Jones, *et al.*, "Segmentation of Confocal Microscope Images of Cell Nuclei in Thick Tissue Sections," J. Microscopy **193**, 212–226 (1999).
25. C. Ortiz de Solorzano, R. Malladi, S. A. Lelievre, and S. J. Lockett, "Segmentation of Nuclei and Cells Using Membrane Related Protein Markers," J. Microscopy **201** (3), 404–415 (2001).
26. T. Pavlidis and Y.-T. Liow, "Integrating Region Growing and Edge Detection," IEEE Trans. Pattern Anal. Machine Intell. **12**, 225–233 (1990).
27. P. Ranefall, B. N. L. Egevad, and E. Bengtsson, "A New Method for Segmentation of Color Images Applied to Immunohistochemically Stained Cell Nuclei," Anal. Cell. Pathol. **15**, 145–156 (1997).
28. P. Ranefall, K. Wester, and E. Bengtsson, "Automatic Quantification of to Immunohistochemically Stained Cell Nuclei Using Unsupervised Image Analysis," Anal. Cell. Pathol. **16**, 29–43 (1998).
29. K. Rodenacker and E. Bengtsson, "A Feature Set for Cytometry on Digitized Microscopic Images," Anal. Cell. Pathol. **25**, 1–36 (2003).
30. B. Roysam, H. Ancin, A. K. Bhattacharjya, *et al.*, "Algorithms for Automated Characterization of Cell Populations in Thick Specimens from 3D Confocal Fluorescence Microscopy Data," J. Microscopy **173**, 115–126 (1994).
31. P. K. Saha, F. W. Wehrli, and B. R. Gomberg, "Fuzzy Distance Transform: Theory, Algorithms, and Applications," Comput. Vision Image Understanding **86** (3), 171–190 (2002).
32. P. K. Sahoo, S. Soltani, A. K. C. Wong, and Y. C. Chen, "A Survey on Thresholding Techniques," Comput. Vision Graph. Image Processing **41**, 233–260 (1988).
33. H. Schulerud and F. Albregtsen, "Many Are Called But Few Are Chosen: Feature Selection and Error Estimation in High-Dimensional Spaces," Comput. Meth. Progr. Biomed. 2003 (in press).

34. N. Sladoje, I. Nyström, and P. K. Saha, "Perimeter and Area Estimations of Digitized Objects with Fuzzy Borders," in *Proc. of the 11th Int. Conf. on Discrete Geometry for Computer Imagery (DGCI), LNCS, Naples, Italy, 2003*, Ed. by I. Nyström, G. Sanniti di Baja, and S. Svensson (Springer, 2003), Vol. 2886, pp. 368–377.

35. P. Soille, *Morphological Image Analysis: Principles and Applications* (Springer, 1999).

36. M. Sonka, V. Hlavac, and R. Boyle, *Image Processing, Analysis and Machine Vision*, 2nd ed. (Brooks/Cole, Pacific Grove, CA, 1999).

37. S. L. Stoev and W. Straßer, "Extracting Regions of Interest Applying Local Watershed Transformation," in *IEEE Visualization 2000, Salt Lake City, 2000*, pp. 21–29.

38. L. Vincent, "Morphological Grayscale Reconstruction in Image Analysis: Applications and Efficient Algorithms," IEEE Trans. Image Processing **2** (2), 176–201 (1993).

39. L. Vincent and P. Soille, "Watershed in Digital Spaces: An Efficient Algorithm Based on Immersion Simulations," IEEE Trans. Pattern Anal. Machine Intell. **13** (6), 583–597 (1991).

40. C. Wählby, F. Erlandsson, K. Nyberg, *et al.*, "Multiple Tissue Antigen Analysis by Sequential Immunofluorescence Staining and Multidimensional Image Analysis," in Proc. of the 12th Scandinavian Conf. on Image Analysis (SCIA), Bergen, Norway, 2001, pp. 25–31.

41. C. Wählby, I.-M. Sintorn, F. Erlandsson, *et al.*, "Combining Intensity, Edge, and Shape Information for 2D and 3D Segmentation of Cell Nuclei on Tissue Sections," J. Microscopy (in press).

42. Q. Yang and B. Parvin, "Chef: Convex Hull of Elliptic Features for 3D Blob Detection," in *Int. Conf. on Pattern Recognition, Québec City, Québec, Canada, 2002*, Ed. by R. Kasturi, D. Laurendeau, and C. Suen (IEEE Computer Society), Vol. II, pp. 282–285.

Ewert Bengtsson. Born 1948. Received his MSci in Engineering Physics in 1974 and his PhD in Physics in 1977, both from Uppsala University. In 1988, adjunct professor and in 1995 full professor in Computerized Image Analysis at Uppsala University. Since 1998, also an adviser to the rector on IT. His research interests include biomedical image analysis, in general, and cell image analysis, in particular. Author of about 130 international reviewed publications in this field.

Carolina Wählby. Born 1974. Received her MSci in Molecular Biotechnology in 1998 and a PhD in Image Analysis in 2003, both from Uppsala University. Currently with the Centre for Image Analysis at Uppsala University, and her interests include development of algorithms for applied digital image cytometry. Author of eight international reviewed publications in this field.

Joakim Lindblad. Born 1973. Received his MSci in Engineering Physics in 1997 and a PhD in Image Analysis in 2003, both from Uppsala University. His research interests include development of general methods for image segmentation, feature extraction, and classification. Currently with the Centre for Image Analysis at Uppsala University working on segmentation of microscopic images of cells in 2D and 3D and development of fast and robust estimators of geometric properties from digital images. Author of seven international reviewed publications in this field.